ORIGINAL RESEARCH

Airway Disease in Children with Primary Ciliary Dyskinesia
Impact of Ciliary Ultrastructure Defect and Genotype

BreAnna Kinghorn[1,2], Margaret Rosenfeld[1,2], Erin Sullivan[1,2], Frankline Onchiri[1,2], Thomas W. Ferkol[3], Scott D. Sagel[4], Sharon D. Dell[5], Carlos Milla[6], Adam J. Shapiro[7], Kelli M. Sullivan[8], Maimoona A. Zariwala[9], Jessica E. Pittman[10], Federico Mollica[11,12], Harm A. W. M. Tiddens[11,12], Mariette Kemner-van de Corput[11,12], Michael R. Knowles[8], Stephanie D. Davis[3], and Margaret W. Leigh[3]; for the Genetic Disorders of Mucociliary Clearance Consortium

[1]Department of Pediatrics, University of Washington School of Medicine, Seattle, Washington; [2]Department of Pediatrics, Seattle Children's Research Institute, Seattle, Washington; [4]Department of Pediatrics, Children's Hospital Colorado, University of Colorado School of Medicine, Aurora, Colorado; [5]Department of Pediatrics, University of British Columbia, Vancouver, British Columbia, Canada; [6]Department of Pediatrics, Stanford University, Palo Alto, California; [7]Department of Pediatrics, McGill University Health Centre Research Institute, Montreal, Quebec, Canada; [8]Pulmonary Medicine Division, [9]Department of Pathology and Laboratory Medicine, Marsico Lung Institute, and [3]Department of Pediatrics, University of North Carolina School of Medicine, Chapel Hill, North Carolina; [10]Department of Pediatrics, Washington University School of Medicine, St. Louis, Missouri; and [11]Department of Pediatric Pulmonology and Allergology, Sophia Children's Hospital, and [12]Department of Pediatric Pulmonology and Allergology, Department of Radiology and Nuclear Medicine, Erasmus Medical Center, Rotterdam, the Netherlands

ORCID IDs: 0000-0002-3522-5387 (B.K.); 0000-0001-6172-4465 (S.D.S.); 0000-0003-2169-9407 (S.D. Dell); 0000-0001-6066-6750 (A.J.S.).

Abstract

Rationale: Primary ciliary dyskinesia (PCD) is characterized by impaired mucociliary clearance, recurrent respiratory infections, progressive airway damage, and obstructive lung disease. Although the association of ciliary ultrastructure defect/genotype with the severity of airflow obstruction has been well characterized, their association with airway abnormalities on chest computed tomography (CT) has been minimally evaluated.

Objectives: We sought to delineate the association of ciliary defect class/genotype with chest CT scores in children with PCD.

Methods: Cross-sectional analysis of children with PCD ($N = 146$) enrolled in a prospective multicenter observational study, stratified by defect type: outer dynein arm (ODA), ODA/inner dynein arm (IDA), IDA/microtubular disorganization (MTD), and normal/near normal ultrastructure with associated genotypes. CTs were scored using the MERAGMA-PCD (Melbourne-Rotterdam Annotated Grid Morphometric Analysis for PCD), evaluating airway abnormalities in a hierarchical order: atelectasis, bronchiectasis, bronchial wall thickening, and mucus plugging/tree-in-bud opacities. The volume fraction of each component was expressed as the percentage of total lung volume. The percentage of disease was computed as the sum of all components. Regression analyses were used to describe the association between clinical predictors and CT scores.

Results: Acceptable chest CTs were obtained in 141 children (71 male): 57 ODA, 20 ODA/IDA, 40 IDA/MTD, and 24 normal/near normal. The mean (standard deviation) age was 8.5 (4.6) years, forced expiratory volume in 1 second (FEV_1) percent predicted was 82.4 (19.5), and %Disease was 4.6 (3.5). Children with IDA/MTD defects had a higher %Disease compared with children with ODA defects (2.71% higher [95% confidence interval (CI), 1.37–4.06; $P < 0.001$]), driven by higher %Mucus plugging (2.35% higher [1.43–3.26; $P < 0.001$]). Increasing age, lower body mass index, and lower FEV_1 were associated with a higher %Disease (0.23%; 95% CI, 0.11–0.35; $P < 0.001$ and 0.03%; 95% CI, 0.01–0.04; $P = 0.008$ and 0.05%; 95% CI, 0.01–0.08; $P = 0.011$, respectively).

Conclusions: Children with IDA/MTD defects had significantly greater airway disease on CT, primarily mucus plugging, compared with children with ODA defects.

Keywords: PCD; bronchiectasis; computed tomography; pediatric lung disease; lung function

(Received in original form June 15, 2022; accepted in final form November 28, 2022)

Supported by the Pathogenesis of PCD Lung Disease (R01HL071798 [M.R.K. and M.A.Z.]); the Genetic Disorders of Mucociliary Clearance Consortium (U54HL096458), a part of the National Center for Advancing Translational Sciences (NCATS) Rare Diseases Clinical Research Network (RDCRN) and supported by the RDCRN Data Management and Coordinating Center (DMCC) (U2CTR002818); and the National Institutes of Health/NCATS Colorado Clinical and Translational Sciences Institute (UL1 TR002535). RDCRN is an initiative of the Office of Rare Diseases Research (ORDR) funded through a collaboration between NCATS and the National Heart, Lung, and Blood Institute (NHLBI).

Ann Am Thorac Soc Vol 20, No 4, pp 539–547, Apr 2023

DOI: 10.1513/AnnalsATS.202206-524OC
Internet address: www.atsjournals.org

Primary ciliary dyskinesia (PCD) is a heterogeneous rare genetic disorder characterized by abnormal ciliary ultrastructure and/or function, leading to impaired mucociliary clearance, recurrent oto-sinopulmonary infections, progressive obstructive airflow limitation, and airway damage (1). The spectrum of airway disease seen on chest computed tomography (CT) among patients with PCD includes atelectasis, bronchiectasis, bronchial wall thickening, and mucus plugging (2).

Pathogenic variants in PCD-related genes cause specific ciliary ultrastructure defects, and genotype–phenotype associations are emerging. In cross-sectional (3, 4) and longitudinal (5) studies, children and young adults with ciliary defects characterized by absent inner dynein arms/microtubular disorganization (IDA/MTD) (75% with biallelic pathogenic variants in *CCDC39*/*CCDC40*) have consistently demonstrated lower growth parameters and spirometric indices than those with other ultrastructural defects. However, the association of ciliary ultrastructure defect/genotype and airway disease on chest CT has been minimally evaluated. Although several groups have assessed the association of lung function parameters (spirometry and lung clearance index) with airway disease identified on chest CT in children with PCD (6–9), these analyses did not stratify by ciliary ultrastructure defect or genotype. Furthermore, these studies were retrospective, and chest CTs were obtained for clinical indications without a standardized procedure.

Our group investigated the association of ciliary ultrastructure defect/genotype and airway disease in children with PCD in a multicenter, prospective observational study including standardized research CTs. Our first report was before the development of an appropriate PCD-specific CT scoring system (3). We described the number of lobes of bronchiectasis and found that in children with PCD between the ages of 5 and 11 years, those with IDA/MTD defects had more lobes with bronchiectasis and alveolar consolidation than those in the combined outer dynein arm (ODA) and ODA/IDA defect groups (3). The primary objective of this current study was to evaluate the association of baseline airway abnormalities on CT with ciliary defect and other clinical characteristics in the same pediatric PCD cohort (3), using the MERAGMA-PCD (Melbourne-Rotterdam Annotated Grid Morphometric Analysis for PCD) hierarchical CT scoring system (10, 11). We hypothesized that the severity of airway abnormalities would be greatest in those individuals with IDA/MTD ciliary ultrastructure defects and corresponding genotypes.

Methods

Study Design and Study Participants

As previously reported, the GDMCC (Genetic Disorders of Mucociliary Clearance Consortium) multicenter, prospective, observational study enrolled participants under 19 years of age with confirmed, probable, or possible PCD at seven research sites between 2006 and 2011 (5). Study subjects were recruited through PCD clinics at the participating sites; referral to these clinics occurred through primary care physicians, pediatric pulmonologists, or self-referral (3). The cohort for this cross-sectional analysis was limited to participants with rigorously confirmed PCD, defined as abnormal ciliary ultrastructure by transmission electron microscopy and/or identification of two pathogenic variants in a PCD-associated gene together with compatible clinical features (12). Clinical and CT data from the first study visit at which a research-quality CT was obtained were used.

Study Procedures

Study procedures have been described previously (3). Briefly, standardized procedures were used for diagnostic testing (evaluation of ciliary ultrastructure and genetic testing for PCD-causing pathogenic variants) (13). Initial study visits included a physical exam, spirometry, respiratory culture (deep oropharyngeal swab or expectorated sputum) and medical history, and chest CT scans according to a standard operating procedure (supplement 1 in the data supplement). Spirometry was performed according to American Thoracic Society guidelines (14). Nasal nitric oxide measurements were performed as previously published (15, 16). Assessments were conducted when participants were at stable baseline and free from acute illness for at least 4 weeks.

CT Scoring

Airway disease was quantified by scoring inspiratory CT scans obtained near total lung capacity with the MERAGMA-PCD scoring system by the Erasmus Medical Center LungAnalysis Core Laboratory. All CT data were deidentified and securely transferred to the LungAnalysis Core Laboratory. The MERAGMA-PCD CT scoring system is a grid-based system adapted from the PRAGMA-CF (Perth-Rotterdam Annotated Grid Morphometric Analysis for Cystic Fibrosis) system (10, 11) developed for quantifying early and advanced cystic fibrosis (CF) lung disease. Scoring was performed using an in-house developed software program (Saldsegvol). A grid was placed on a stratified random selection of 10 axial equally spaced CT slices of inspiratory scans, and the lung tissue in each grid box was annotated

Author Contributions: All authors have given approval to the final version of this manuscript. B.K.: conception of design, acquisition of data, analysis design and interpretation of data, and writing of the manuscript. M.R.: conception of design, acquisition of data, analysis design and interpretation of data, and review of the manuscript. E.S. and F.O.: biostatistician, analysis design, interpretation of data, and development of tables and figures. T.W.F., S.D.S., S.D. Dell, C.M., A.J.S., K.M.S., M.A.Z., J.E.P., and M.K.-v.d.C.: conception of design, acquisition of data, and manuscript review. F.M.: conception of design, acquisition of data, interpretation of data, computed tomography (CT) scoring certified observer, interpretation of data, and manuscript review. H.A.W.M.T. and M.K.-v.d.C.: conception of design, CT scoring, interpretation of data, and manuscript review. S.D. Davis: conception of design, analysis design, and manuscript review. M.W.L.: conception of design, acquisition of data, analysis design, and review of the manuscript.

Correspondence and requests for reprints should be addressed to BreAnna Kinghorn, M.D., M.S., Pulmonary and Sleep Medicine Division, Seattle Children's Hospital, OC.7.720, 4800 Sand Point Way NE, Seattle, WA 98105. E-mail: breanna.kinghorn@seattlechildrens.org.

This article has a related editorial.

This article has a data supplement, which is accessible from this issue's table of contents at www.atsjournals.org.

for abnormalities in the following hierarchical order: atelectasis (with or without included bronchiectasis), bronchiectasis (outer edge bronchus artery cross-sectional area ratio greater than one), bronchial wall thickening (airway walls thicker and/or have increased signal intensity relative to normal airways, assessed subjectively), and mucus plugging (including tree-in-bud densities). The volume fraction of each scored component was expressed as a percentage of total lung volume. The composite score %Disease was computed as the sum of %Atelectasis, %Bronchiectasis, %Airway wall thickening, and %Mucus plugging. Primary outcome measures were %Disease and %Bronchiectasis; other component scores were examined as secondary endpoints. Expiratory scans were only obtained in 43% (number of expiratory scans = 60) of participants, so trapped air (which is assessed on expiratory scans) was not evaluated. Image quality was assessed, and CTs were considered invalid and excluded from analyses if the scan contained less than 10 slices, presented incidental findings and acute conditions relevant for the participants, presented big slice intervals between slices, or were not properly uploaded to the annotation software. All CT scans were annotated by one blinded observer (F.M.) trained and certified in both PRAGMA-CF and MERAGMA-PCD scoring. Intraobserver consistency (ICC) scores and interrater reliability were calculated by having 25 CT scans (roughly 10% of the cohort) scored for a second time after a 1-month time interval by the same observer in a blinded fashion, as well as scored by a second observer. ICC and interrater reliability for MERAGMA-PCD scores were assessed by a two-way mixed effects model. An ICC higher than 0.8 was rated as excellent; between 0.6 and 0.8 was rated as good; between 0.4 and 0.6 was rated as moderate; and lower than 0.4 was considered poor.

Statistical Analysis

Ciliary ultrastructure defects were classified as *1*) IDA/MTD; *2*) ODA/IDA; *3*) ODA; and *4*) normal or near normal ciliary structure (5). Demographic and clinical characteristics at the time of the CT scan were summarized descriptively by defect group. Growth parameters (height, weight, and body mass index [BMI]) were derived from the Centers for Disease Control and Prevention reference data (17). Spirometry values were expressed as percent predicted on the basis of the Global Lung Initiative reference equations (18). Continuous variables were assessed for normality using quantile–quantile plots and histograms and summarized using means and standard deviations or medians and interquartile ranges, as appropriate. Linear regression was used to assess the association between CT score and ultrastructure ciliary defect adjusted for age and sex and illustrated by forest plots. ODA was chosen as the reference group because it was the largest defect group. The association of CT score with clinical predictors at the time of scan (spirometry, growth parameters, and respiratory culture

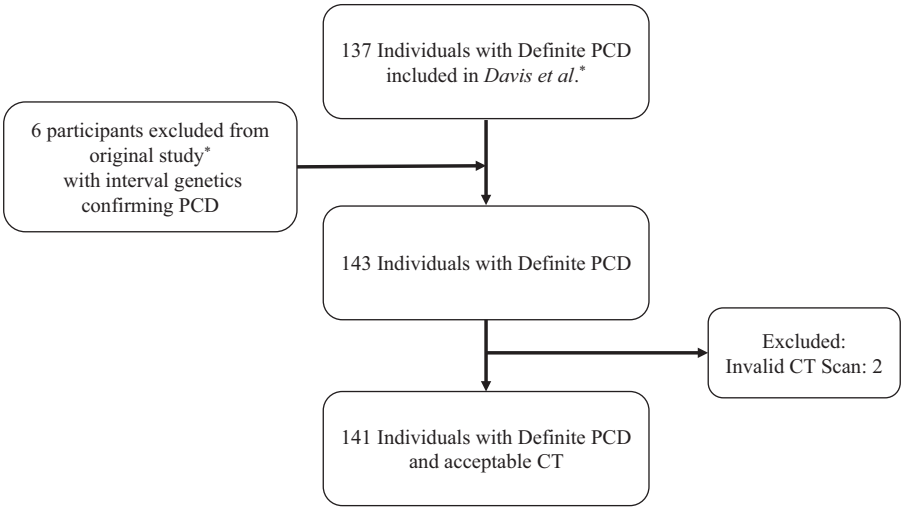

Figure 1. Flow chart outlining the enrolled participants. *Definite primary ciliary dyskinesia (PCD) is defined as abnormal ciliary ultrastructure by transmission electron microscopy and/or identification of two pathogenic variants in a PCD-associated gene together with compatible clinical features (Davis and colleagues [5]). CT = computed tomography.

Table 1. Ultrastructural and genetic findings

PCD-causing Gene	ODA	ODA/IDA	IDA/MTD	Normal/Near Normal	Total
None identified	—	1	1	—	2
DNAH5	40	—	—	—	40
DNAI1	9	—	—	—	9
DNAI2	5	—	—	—	5
CCDC114	2	—	—	—	2
ARMC4	1	—	—	—	1
LRRC6	—	3	—	—	3
DNAAF4 (DYX1C1)	—	3	—	—	3
CCDC103	—	2	—	—	2
DNAAF4 (HEATR2)	—	2	—	—	2
SPAG1	—	2	—	—	2
DNAAF1(LRRC50)	—	2	—	—	2
DNAAF2 (KTU)	—	1	—	—	1
DNAAF3	—	2	—	—	2
PIH1D3 (X-linked)	—	1	—	—	1
CCDC40	—	—	21	—	21
CCDC39	—	—	18	—	18
DNAH11	—	—	—	11	11
RPGR (X-linked)	—	—	—	1	1
CCNO	—	—	—	4	4
RSPH4A	—	—	—	3	3
RSPH1	—	—	—	1	1
RSPH9	—	—	—	1	1
HYDIN	—	—	—	3	3
PIK3CD	—	1	—	0	1
Total	57	20	40	24	141

Definition of abbreviations: IDA = inner dynein arm; MTD = microtubular disorganization; ODA = outer dynein arm; PCD = primary ciliary dyskinesia.

positive for *Pseudomonas aeruginosa*) was assessed with linear regression adjusting for ultrastructure defect group, sex, and age. All estimates are presented with 95% confidence intervals (CIs). Two-sided *P* values less than 0.05 were considered statistically significant. We did not correct for multiple comparisons. Analyses were performed using SAS version 9.4.

Ethics Approval

Institutional review board approval was obtained at each site. Informed consent was obtained from parents/guardians and assent from participants as appropriate. An observational safety monitoring board reviewed and approved all protocols.

Results

Participant Characteristics

The cohort included the original 137 participants described by Davis and colleagues (5), as well as six participants with interval genetic testing confirming the diagnosis of PCD. Of the 143 participants with a definite diagnosis of PCD, 141 had an acceptable baseline ($n = 130$) or second-visit CT scan (if no chest CT was performed at the baseline visit, $n = 11$) and comprised the analytic cohort (Figure 1). ICC scores were excellent for %Atelectasis (0.87), %Mucus plugging (0.99), and %Disease (0.96), moderate for %Bronchiectasis (0.58), and poor for %Airway wall thickening (0.05), which was likely because of the small amount of %Airway wall thickening. The ciliary ultrastructural defects and associated

Table 2. Baseline demographics and clinical characteristics of 141 children with primary ciliary dyskinesia, stratified by ciliary ultrastructural defect group

	All ($n = 141$)	ODA ($n = 57$)	ODA/IDA ($n = 20$)	IDA/MTD ($n = 40$)	Normal/Near Normal ($n = 24$)
Demographics					
Male, *n* (%)	71 (50.4)	29 (50.9)	12 (60.0)	21 (52.5)	9 (37.5)
Age (yr) at diagnosis, mean (SD), range	3.9 (3.8) (0.1–14.0)	4.8 (4.4) (0.1–14.0)	3.2 (3.4) (0.1–10.0)	2.5 (2.9) (0.1–13.0)	5.2 (2.9) (1.5–10.0)
Age (yr) at CT scan, mean (SD), range	8.5 (4.6) (0.4–18.5)	9.5 (4.2) (0.4–18.2)	8.0 (5.6) (0.7–17.3)	6.9 (4.4) (0.5–16.5)	9.1 (4.6) (1.5–18.5)
Race/ethnicity, *n* (%)					
Hispanic	14 (9.9)	3 (5.3)	1 (5.0)	5 (12.5)	5 (20.8)
American Indian/Alaska Native	1 (0.7)	1 (1.8)	0 (0.0)	0 (0.0)	0 (0.0)
Asian	13 (9.2)	4 (7.0)	5 (25.0)	3 (7.5)	1 (4.2)
Black	4 (2.8)	1 (1.8)	1 (5.0)	2 (5.0)	0 (0.0)
White	105 (74.5)	46 (80.7)	13 (65.0)	29 (72.5)	17 (70.8)
Identified as >1	4 (2.8)	2 (3.5)	0 (0.0)	1 (2.5)	1 (4.2)
Growth parameters, mean (SD)*					
Weight percentile	49.5 (31.8)	59.0 (32.9)	48.0 (34.7)	37.0 (24.0)	48.9 (32.2)
Height percentile	44.5 (29.4)	50.1 (30.6)	46.3 (30.1)	38.5 (24.8)	39.8 (32.3)
BMI percentile	54.2 (30.8)	61.3 (29.8)	49.3 (35.1)	45.1 (26.0)	54.6 (34.4)
Spirometry†					
FVC, % predicted (SD)	94.0 (18.1)	99.3 (17.3)	85.2 (20.8)	84.6 (18.7)	96.5 (10.9)
FEV_1, % predicted (SD)	82.4 (19.5)	87.9 (17.8)	81.0 (22.7)	68.9 (18.9)	84.8 (15.3)
FEV_1/FVC (SD)	87.1 (11.0)	87.9 (9.0)	94.3 (10.0)	80.7 (10.6)	87.6 (13.9)
$FEF_{25–75}$, % predicted (SD)	63.7 (27.5)	67.9 (24.2)	71.8 (28.6)	45.1 (21.7)	69.5 (34.2)
Diagnostics†					
Nasal nitric oxide, nl/min mean (IQR)	14.3 (10.1–18.9)	13.7 (6.8–17.1)	12.8 (10.6–22.1)	14.0 (8.5–25.0)	17.7 (12.0–27.5)
Clinical features, *n* (%)					
Neonatal respiratory distress	117 (83.0)	45 (78.9)	18 (90.0)	36 (90.0)	18 (75.0)
Laterality defect	69 (52.3)	32 (58.2)	10 (50.0)	20 (51.3)	7 (38.9)
Chronic year-round wet cough	140 (99.3)	57 (100.0)	20 (100.0)	39 (97.5)	24 (100.0)
Chronic year-round nasal congestion	138 (97.9)	56 (98.2)	19 (95.0)	40 (100.0)	23 (95.8)
Chronic otitis media	132 (93.6)	54 (94.7)	18 (90.0)	37 (92.5)	23 (95.8)
Microbiology, *n* (%)‡					
No growth	11 (7.8)	2 (3.5)	1 (5.0)	3 (7.5)	5 (20.8)
Pseudomonas aeruginosa	10 (7.1)	3 (5.3)	0 (0.0)	4 (10.0)	3 (12.5)
Haemophilus influenzae	65 (46.1)	25 (43.9)	8 (40.0)	22 (55.0)	10 (41.7)
Staphylococcus aureus	45 (31.9)	19 (33.3)	7 (35.0)	13 (32.5)	6 (25.0)
Streptococcus pneumoniae	32 (22.7)	17 (29.8)	6 (30.0)	6 (15.0)	3 (12.5)
Moraxella catarrhalis	20 (14.2)	11 (19.3)	3 (15.0)	3 (7.5)	3 (12.5)
Non-tuberculous mycobacteria	6 (4.3)	2 (3.5)	1 (5.0)	2 (5.0)	1 (4.2)

Definition of abbreviations: BMI = body mass index; CT = computed tomography; $FEF_{25–75}$ = forced midexpiratory flow; FEV_1 = forced expiratory volume in 1 second; FVC = forced vital capacity; IDA = inner dynein arm; IQR = interquartile range; MTD = microtubular disorganization; ODA = outer dynein arm; SD = standard deviation.

*Weight, height, and BMI were derived from the Centers for Disease Control and Prevention reference data (17).

†Spirometry data were available in 83/87 participants ages 6 years and older, nasal nitric oxide concentrations were available in 101/105 participants ages 5 years and older, and data on laterality defect were available in 132/141 participants. BMI is calculated for children ages 2 years and older ($n = 127$).

‡Sputum culture obtained at the initial study visit was obtained via throat swab (55) or expectorate sputum sample (86).

genotypes (two pathogenic or likely pathogenic variants in a known PCD-associated gene; or, for X-linked cases, one pathogenic variant in the X chromosome gene in males) are shown in Table 1. The normal/near normal cohort included children with normal ciliary ultrastructure on electron microscopy (EM) (*DNAH11* and *RPGR*), as well as children with subtle ciliary defects on EM, including central apparatus and radial spoke defects (*RSPH4A*, *RSPH1*, *RSPH9*, and *HYDIN*), and children with absent or reduced cilia (*CCNO*) (Table 1). Baseline characteristics categorized by ciliary ultrastructure defect are shown in Table 2. The mean (standard deviation [SD]) age of the cohort was 8.5 (4.6) years. The 40 participants with IDA/MTD ciliary ultrastructure defects were, on average, younger with lower growth parameters and spirometric parameters compared with participants with other defects. As expected, about half of the participants had a laterality defect. Isolation of *P. aeruginosa* from respiratory cultures was rare at the baseline/second visit, occurring in 7% of the cohort.

Spectrum of Airway Abnormalities

Airway disease severity varied widely, as illustrated in the stacked bar plots of CT scores (Figure 2). CT scores stratified by the ciliary ultrastructure defect group are shown in Table 3. Mean (SD, range) %Disease for the cohort was 4.6% (3.5, 0.2–19.6), with %Atelectasis and %Bronchiectasis being the primary contributors (1.6% [1.8, 1–15.2] and 1.5% [0.9, 0–4.1], respectively). Children with IDA/MTD ciliary ultrastructure defects had the highest mean (SD, range) %Disease at

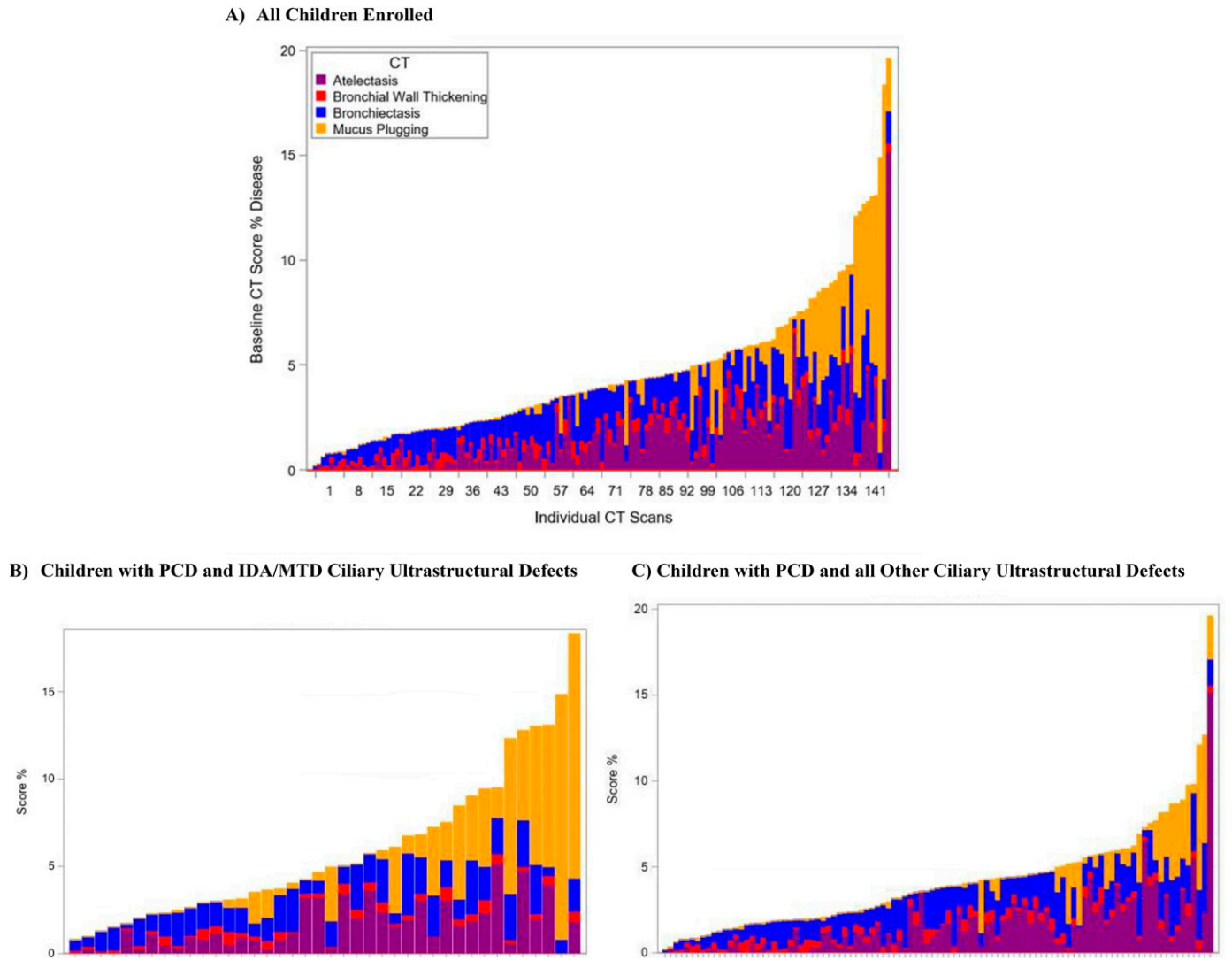

Figure 2. Spectrum of disease scores in 141 children with primary ciliary dyskinesia (PCD) using the (*A*) Melbourne-Rotterdam annotated grid morphometric analysis (MERAGMA)-PCD CT scoring system and (*B*) stratified by ciliary ultrastructural defect inner dynein arm/microtubular disorganization (IDA/MTD) versus (*C*) other. Stacked bar plots showing the wide spectrum of disease scores found by the MERAGMA-PCD scoring system. Participants are sorted on the basis of the total score percentage. %Disease for each patient is subdivided by the subscores %Bronchiectasis, %Mucus plugging, %Airway wall thickening, and %Atelectasis. (*A*) All children enrolled. (*B*) Children with PCD and IDA/MTD ciliary ultrastructural defects. (*C*) Children with PCD and all other ciliary ultrastructural defects. CT = computed tomography.

Table 3. Baseline computed tomography scores in 141 children with primary ciliary dyskinesia, stratified by ciliary ultrastructural defect group

	All ($N = 141$)	ODA ($n = 57$)	ODA/IDA ($n = 20$)	IDA/MTD ($n = 40$)	Normal/Near Normal ($n = 24$)
Atelectasis (%), mean (SD), range	1.6 (1.8) 1–15.2	1.4 (1.3) 0–5.6	1.7 (1.7) 0–6.6	1.6 (1.4) 0–15.2	1.7 (3.1) 0–15.2
Bronchiectasis (%), mean (SD), range	1.5 (0.9) 0–4.1	1.6 (0.9) 0.2–4.1	1.7 (0.8) 0.4–2.9	1.6 (0.8) 0.2–3.6	1.2 (1.0) 0–3.5
Bronchial wall thickening (%), mean (SD), range	0.4 (0.2) 0–1.0	0.4 (0.2) 0–0.8	0.5 (0.2) 0.2–1.0	0.3 (0.2) 0.1–0.7	0.3 (0.2) 0–0.8
Mucus plugging (%), mean (SD), range	1.2 (2.4) 0–14.0	0.5 (1.1) 0–6.2	0.9 (2.1) 0–8.4	2.3 (3.7) 0–14	1.1 (1.6) 0–4.6
Disease (%)*, mean (SD), range	4.6 (3.5) 0.2–19.6	3.8 (2.4) 0.6–12.7	4.7 (2.9) 0.9–12.1	5.9 (4.3) 0.8–18.3	4.3 (4.1) 0.2–19.6

Definition of abbreviations: IDA = inner dynein arm; MTD = microtubular disorganization; ODA = outer dynein arm; SD = standard deviation.
*Disease (%) is the sum of atelectasis (%), bronchiectasis (%), airway wall thickening (%), and mucus plugging (%).

5.9% (4.3, 0.8–18.3), with %Mucus plugging identified as the greatest component at 2.3% (3.7, 0–14).

Association of Ciliary Ultrastructure Defect with Airway Disease

In linear regression models, children with IDA/MTD defects had significantly higher mean %Disease compared with children with ODA defects (reference group) after adjustment for age and sex (2.71% higher; 95% CI, 1.37–4.06; $P < 0.001$) (Figure 3). This difference was predominantly driven by higher mean %Mucus plugging (2.35% higher; 95% CI, 1.43–3.26; $P < 0.001$). There were no differences in %Disease or subscores between children with ODA and either ODA/IDA or normal/near normal ultrastructure (Figure 3).

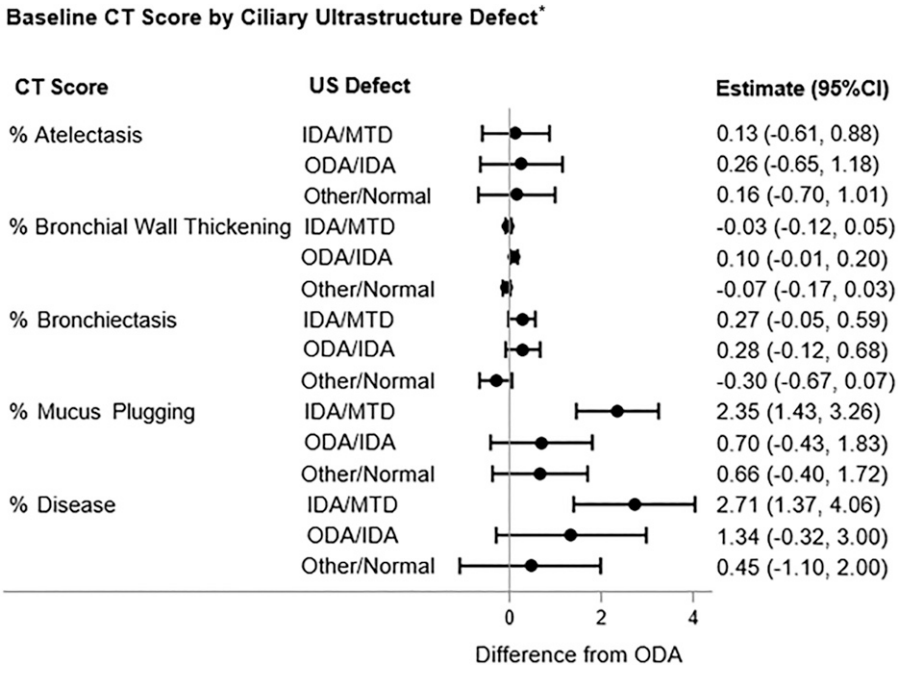

Figure 3. Forest plots demonstrating the association between airway abnormalities on the basis of Melbourne-Rotterdam annotated grid morphometric analysis for primary ciliary dyskinesia (PCD) CT scores and ciliary ultrastructural defect* in 141 children with PCD. *Ciliary ultrastructural defect reference group ODA. Adjusted for age and sex. CI = confidence interval; CT = computed tomography; IDA = inner dynein arm; MTD = microtubular disorganization; ODA = outer dynein arm; US = ultrastructure.

Association of Clinical Characteristics with Airway Disease

Increasing age was associated with a higher mean %Disease of 0.23% per year of age (95% CI, 0.11–0.35; $P < 0.001$), higher %Bronchiectasis (per year age) of 0.08% (95% CI, 0.05–0.11; $P < 0.001$), and higher %Mucous plugging (per year of age) of 0.18% (95% CI, 0.09–0.26; $P < 0.001$) (Table 4), after adjusting for defect group and sex. Sex was not associated with any of the CT outcome measures.

Lower body mass index percentile was associated with higher mean %Disease (0.03% increase, 95% CI, 0.01–0.04; $P = 0.008$) and %Atelectasis (0.01% increase; 95% CI, 0.002–0.02; $P = 0.017$) (Table 4), independent of the effect of defect group, age, and sex. Height and weight percentile were not associated with any of the CT score components. A history of neonatal respiratory distress was not associated with any of the CT scoring components.

Lower forced expiratory volume in 1 second (FEV_1) percent predicted was associated with higher mean %Disease (0.05% higher; 95% CI, 0.01–0.08; $P = 0.011$), %Atelectasis (0.02% higher; 95% CI, 0.0–0.04; $P = 0.004$), and %Mucus plugging (0.03% higher; 95% CI, 0.001–0.006; $P = 0.046$) (Table 4). Lower forced vital capacity (FVC) percent predicted was associated with higher mean %Disease (0.07% higher; 95% CI, 0.03–0.10; $P < 0.001$), primarily driven by an increase in %Atelectasis (0.03% higher; 95% CI, 0.01–0.04; $P < 0.001$). Higher FEV_1/FVC and forced midexpiratory flow were associated with increased %Bronchiectasis (0.03% higher; 95% CI, 0.010–0.046;

Table 4. Association of growth parameters, spirometry, and microbiology with baseline computed tomography scores from linear regression models in 141 children with primary ciliary dyskinesia*

	Atelectasis (%)	Bronchiectasis (%)	Bronchial Wall Thickening (%)	Mucus Plugging (%)	Disease (%)
Demographics					
Age, yr	−0.028 (−0.094 to 0.037)	0.081 (0.053 to 0.110)†	0.001 (−0.007 to 0.008)	0.176 (0.095 to 0.257)†	0.230 (0.111 to 0.349)†
Growth parameters					
Weight (%)	−0.009 (−0.018 to 0.001)	−0.002 (−0.007 to 0.002)	0.001 (0.000 to 0.002)	−0.003 (−0.015 to 0.009)	−0.013 (−0.031 to 0.005)
Height (%)	−0.002 (−0.012 to 0.008)	0.002 (−0.003 to 0.006)	0.001 (0.000 to 0.002)	0.003 (−0.009 to 0.016)	0.004 (−0.014 to 0.023)
BMI (%)	−0.012 (−0.023 to −0.002)†	−0.003 (−0.008 to 0.002)	0.001 (0.000 to 0.003)†	−0.012 (−0.025 to 0.002)	−0.026 (−0.045 to −0.007)†
Spirometry‡					
FVC, % predicted	−0.027 (−0.043 to −0.012)†	−0.008 (−0.019 to 0.004)	0.000 (−0.002 to 0.003)	−0.032 (−0.062 to −0.001)†	−0.067 (−0.104 to −0.029)†
FEV_1, % predicted	−0.022 (−0.037 to −0.007)†	0.003 (−0.008 to 0.014)	0.001 (−0.002 to 0.003)	−0.029 (−0.058 to −0.001)†	−0.048 (−0.084 to −0.011)†
FEV_1/FVC	0.000 (−0.027 to 0.026)	0.028 (0.010 to 0.046)†	0.002 (−0.002 to 0.006)	−0.026 (−0.076 to 0.024)	0.004 (−0.060 to 0.069)
$FEF_{25–75}$, % predicted	−0.009 (−0.020 to 0.001)	0.009 (0.001 to 0.016)†	0.000 (−0.001 to 0.002)	−0.014 (−0.034 to 0.007)	−0.014 (−0.040 to 0.012)
Microbiology					
Pseudomonas aeruginosa§	0.565 (−0.612 to 1.742)	0.218 (−0.292 to 0.728)	−0.048 (−0.184 to 0.089)	1.211 (−0.232 to 2.654)	1.947 (−0.164 to 4.058)

Definition of abbreviations: BMI = body mass index; $FEF_{25–75}$ = forced midexpiratory flow; FEV_1 = forced expiratory volume in 1 second; FVC = forced vital capacity.
*Linear regression model adjusted for ciliary ultrastructural defect, age, and sex.
†$P < 0.05$.
‡Spirometry data are available in 83/87 children with primary ciliary dyskinesia ages 6 years and older.
§*P. aeruginosa* was identified in 20 participants.

$P = 0.002$ and 0.009% higher; 95% CI, 0.001–0.016; $P = 0.021$, respectively), yet were not associated with other CT score components. We did not find any relationship between the isolation of *P. aeruginosa* from respiratory culture and %Disease or other CT components, but, as stated above, only 7% of participants had positive cultures at the baseline/second visit (Table 4).

Discussion

In this North American cohort of children and young adults with confirmed PCD, IDA/MTD defects (associated with pathogenic variants in *CCDC39* and *CCDC40*) were associated with more severe airway disease than ODA defects, driven by greater mucus plugging. We also found that increased age and lower spirometric indices (FEV_1 and FVC) were associated with greater airway disease. In a prior longitudinal evaluation of the current cohort, FEV_1 declined significantly with age, with children with IDA/MTD defects having the greatest rate of decline (5). Taken together, these studies suggest that both lung function and airway disease are progressive in PCD and more severe in those with IDA/MTD defects.

Our observation of greater mucus plugging associated with IDA/MTD defects is novel and could shed light on the underlying mechanism of airway disease in PCD, particularly in those with IDA/MTD defects. Cilia on respiratory epithelial cells are involved in a mechanosensory feedback mechanism in which sensing of increased mucus load leads to the release of adenosine triphosphate (ATP) with a corresponding increase in airway surface liquid and enhanced mucociliary clearance (19, 20). *CCDC39* and *CCDC40* function as ciliary rulers directing the spacing and arrangement of the IDA and radial spokes and are integral components of the nexin–dynein regulatory complex (21–23). Severe disruption in cilia structure, as seen with IDA/MTD defects, could lead to a loss of the feedback mechanism and lead to mucus layer collapse on the cilia with associated increased mucus plugging.

The contribution of mucus plugging to other airway diseases, including asthma (24, 25) and chronic obstructive pulmonary disease (24), is receiving growing recognition. In the Severe Asthma Research Program cohort, mucus plugs on CT were

common and associated with lower FEV_1 and ventilation defects (25, 26). In longitudinal analyses of that cohort, change in mucus plug score negatively correlated with changes in FEV_1 and positively correlated with CT air trapping (27). Preliminary evidence suggests that mucus plugging in asthma may be mediated through pathologically relevant changes in MUC5AC and MUC5B in the airway mucus gel (28). The role of mucus plugging in PCD airway disease deserves further investigation.

Several prior studies have described airway disease in PCD and evaluated its association with lung function (3, 6–9, 29). Our study adds to this knowledge base by evaluating the association of ciliary ultrastructure/genotype with airway disease severity and using the MERAGMA-PCD scoring system, allowing assessment of the contribution of bronchiectasis, mucus plugging, atelectasis, and bronchial wall thickening to the overall extent of disease. We found that lower spirometric indices (FEV_1 and FVC) were associated with greater airway disease on chest CT (adjusting for ciliary ultrastructure defect group and age), with lower FEV_1 associated with both increased atelectasis and mucus plugging, and lower FVC associated with increased atelectasis. We included only CTs obtained during stable respiratory baseline (at least 4 weeks after respiratory illness), so these results suggest that consideration should be given to imaging to evaluate for clinically silent atelectasis in patients with reduced FEV_1 or FVC not associated with acute respiratory illnesses. Surprisingly, we found that higher FEV_1/FVC and (to a lesser extent) forced midexpiratory flow percent predicted values were associated with higher %Bronchiectasis. The reason for this observed association is unclear as it lacks biological plausibility and would be unlikely to be replicated in another cohort.

We used the novel MERAGMA-PCD CT scoring system to characterize airway disease. Prior studies have extrapolated CT scoring systems developed for CF to PCD, including the modified Brody score (9, 30), the Bhalla scoring system (7, 31), and the CF CT score (32). These studies assumed that the underlying pathophysiology of CF and PCD are similar. In fact, individuals with PCD are more likely to have mucus plugging, lobar atelectasis, air trapping, and tree-in-bud densities than those with CF (2). The MERAGMA-PCD CT scoring system, though adapted from a CF scoring system (10, 11), was specifically developed on the basis of CT scans from patients with PCD to account for atelectasis with or without bronchiectasis and for tree-in-bud densities.

To understand the differences in %Disease between the ciliary ultrastructure groups from a clinical perspective, it is important to acknowledge that airways only occupy 0.10–0.25% of total lung volume in children aged 6–16 years with normal chest CTs (data not shown). Because the PRAGMA and MERAGMA scoring systems only evaluate airway disease, %Disease values are anticipated to be very small, even in individuals with more advanced disease. To illustrate this, we randomly selected CTs from children with mild, moderate, and severe disease. The number of diseased airways in the child with mild disease (%Disease, 1.2%) was 39 (23%) of 170 visible airways, compared with the child with moderate disease (%Disease, 3.6%) with 107 (40%) diseased airways of 268 visible airways. The child with severe disease (%Disease, 8.7%) had 578 (82%) diseased airways out of 708 visible airways. Data on the longitudinal progression of CT scores in PCD are lacking. However, in CF cohorts, the mean annual progression of %Disease using PRAGMA-CF CT scores has ranged from 0.5% per year to 1.23% per year, depending on the age of the cohort (33). In the Saline Hypertonic in Preschoolers (SHIP)-CT study, (34) randomized controlled trial of inhaled hypertonic saline in preschool children with CF, the estimated treatment effect on %Disease was 0.67%. In the current cohort, children with IDA/MTD defects had an estimated 2.1% higher mean %Disease compared with children with ODA defects, representing a substantial difference in the severity of airway disease. When adjusting for ciliary ultrastructure defect, we found that a 10% decline in FEV_1 was associated with a 0.48% increase in %Disease.

Limitations

Our study has several limitations. This study's cross-sectional design precludes us from addressing the longitudinal progression of airway disease. Our classification of the PCD population on the basis of the ciliary ultrastructural defect and associated pathogenic variants is likely an oversimplified approach. Molecular phenotyping might better encompass the complex interplay between ciliary assembly and clinical phenotype in PCD, but no such phenotyping framework exists currently. The MERAGMA-PCD scoring system is hierarchical, prohibiting the assessment of all CT score components in a given region of the lung, and may underestimate the extent of airway disease. We were unable to score air trapping, as there were too few expiratory scans that met the acceptability criteria. We lacked sufficiently detailed data on treatments to evaluate the association of treatments with CT scores. There are potential confounders not captured in our data, such as social determinants of health (race/ethnicity, socioeconomic status, and access to care). Lastly, the relatively small size of each defect group limited our power to detect certain differences between groups in CT score components. To better understand the progression of lung disease and its association with ciliary ultrastructure defect, we plan to use this same PCD cohort to evaluate disease progression over a 10-year period.

Conclusions

Our study reinforces the progressive nature of PCD lung disease and the more severe phenotype associated with IDA/MTD ultrastructure defects (pathogenic variants in *CCDC39* and *CCDC40*). These children and young adults have a significantly greater extent of airway abnormalities, specifically greater mucus plugging, raising concerns related to mucus layer–ciliary interactions essential for hydrating the periciliary layer and allowing for effective mucociliary clearance. Identification of high-risk children is essential for early intervention opportunities; therapeutic development aimed at these proposed mechanisms could improve outcomes in PCD. ■

Author disclosures are available with the text of this article at www.atsjournals.org.

Acknowledgment: The authors thank Dr. Jaclyn Stonebraker and Elizabeth Schecterman for technical assistance and Dr. Hong Dang for the bioinformatics assistance. The authors thank Dr. Shrikant Mane and Dr. Francesc Lopez-Giraldez from the Yale Center for Mendelian Genomics (UM1 HG006504) for providing whole exome sequencing and bioinformatics support.

References

1 Leigh MW, Horani A, Kinghorn B, O'Connor MG, Zariwala MA, Knowles MR. Primary ciliary dyskinesia (PCD): a genetic disorder of motile cilia. *Transl Sci Rare Dis* 2019;4:51–75.
2 Tadd K, Morgan L, Rosenow T, Schultz A, Susanto C, Murray C, *et al.* CF derived scoring systems do not fully describe the range of structural changes seen on CT scans in PCD. *Pediatr Pulmonol* 2019;54: 471–477.
3 Davis SD, Ferkol TW, Rosenfeld M, Lee HS, Dell SD, Sagel SD, *et al.* Clinical features of childhood primary ciliary dyskinesia by genotype and ultrastructural phenotype. *Am J Respir Crit Care Med* 2015;191: 316–324.
4 Shoemark A, Rubbo B, Legendre M, Fassad MR, Haarman EG, Best S, *et al.* Topological data analysis reveals genotype-phenotype relationships in primary ciliary dyskinesia. *Eur Respir J* 2021;58: 2002359.
5 Davis SD, Rosenfeld M, Lee HS, Ferkol TW, Sagel SD, Dell SD, *et al.* Primary ciliary dyskinesia: longitudinal study of lung disease by ultrastructure defect and genotype. *Am J Respir Crit Care Med* 2019; 199:190–198.
6 Maglione M, Montella S, Santamaria F. Chest CTs in primary ciliary dyskinesia: not too few, but not too many! *Pediatr Pulmonol* 2012;47: 733–735.
7 Magnin ML, Cros P, Beydon N, Mahloul M, Tamalet A, Escudier E, *et al.* Longitudinal lung function and structural changes in children with primary ciliary dyskinesia. *Pediatr Pulmonol* 2012;47:816–825.
8 Boon M, Vermeulen FL, Gysemans W, Proesmans M, Jorissen M, De Boeck K. Lung structure-function correlation in patients with primary ciliary dyskinesia. *Thorax* 2015;70:339–345.
9 Santamaria F, Montella S, Tiddens HAWM, Guidi G, Casotti V, Maglione M, *et al.* Structural and functional lung disease in primary ciliary dyskinesia. *Chest* 2008;134:351–357.
10 Rosenow T, Oudraad MC, Murray CP, Turkovic L, Kuo W, de Bruijne M, *et al.*; Australian Respiratory Early Surveillance Team for Cystic Fibrosis (AREST CF). PRAGMA-CF. A quantitative structural lung disease computed tomography outcome in young children with cystic fibrosis. *Am J Respir Crit Care Med* 2015;191:1158–1165.
11 Loeve M, Hop WC, de Bruijne M, van Hal PT, Robinson P, Aitken ML, *et al.*; Computed Tomography Cystic Fibrosis Survival Study Group. Chest computed tomography scores are predictive of survival in patients with cystic fibrosis awaiting lung transplantation. *Am J Respir Crit Care Med* 2012;185:1096–1103.
12 Shapiro AJ, Davis SD, Polineni D, Manion M, Rosenfeld M, Dell SD, *et al.*; American Thoracic Society Assembly on Pediatrics. Diagnosis of primary ciliary dyskinesia. An official American Thoracic Society clinical practice guideline. *Am J Respir Crit Care Med* 2018;197: e24–e39.
13 Shapiro AJ, Zariwala MA, Ferkol T, Davis SD, Sagel SD, Dell SD, *et al.*; Genetic Disorders of Mucociliary Clearance Consortium. Diagnosis, monitoring, and treatment of primary ciliary dyskinesia: PCD foundation consensus recommendations based on state of the art review. *Pediatr Pulmonol* 2016;51:115–132.
14 Miller MR, Hankinson J, Brusasco V, Burgos F, Casaburi R, Coates A, *et al.*; ATS/ERS Task Force. Standardisation of spirometry. *Eur Respir J* 2005;26:319–338.
15 Leigh MW, Hazucha MJ, Chawla KK, Baker BR, Shapiro AJ, Brown DE, *et al.* Standardizing nasal nitric oxide measurement as a test for primary ciliary dyskinesia. *Ann Am Thorac Soc* 2013;10:574–581.
16 Shapiro AJ, Dell SD, Gaston B, O'Connor M, Marozkina N, Manion M, *et al.* Nasal nitric oxide measurement in primary ciliary dyskinesia. A technical paper on standardized testing protocols. *Ann Am Thorac Soc* 2020;17:e1–e12.
17 Centers for Disease Control and Prevention. A SAS program for the 2000 CDC growth charts (ages 0 to $<$ 20 years). 2016 [accessed 2020 Jan 21]. Available from: https://www.cdc.gov/nccdphp/dnpao/growthcharts/resources/sas.htm.
18 Quanjer PH, Stanojevic S, Cole TJ, Baur X, Hall GL, Culver BH, *et al.*; ERS Global Lung Function Initiative. Multi-ethnic reference values for spirometry for the 3-95-yr age range: the global lung function 2012 equations. *Eur Respir J* 2012;40:1324–1343.
19 Button B, Okada SF, Frederick CB, Thelin WR, Boucher RC. Mechanosensitive ATP release maintains proper mucus hydration of airways. *Sci Signal* 2013;6:ra46.
20 Liu L, Shastry S, Byan-Parker S, Houser G, Chu KK, Birket SE, *et al.* An autoregulatory mechanism governing mucociliary transport is sensitive to mucus load. *Am J Respir Cell Mol Biol* 2014;51:485–493.
21 Oda T, Yanagisawa H, Kamiya R, Kikkawa M. A molecular ruler determines the repeat length in eukaryotic cilia and flagella. *Science* 2014;346:857–860.
22 Merveille AC, Davis EE, Becker-Heck A, Legendre M, Amirav I, Bataille G, *et al.* CCDC39 is required for assembly of inner dynein arms and the dynein regulatory complex and for normal ciliary motility in humans and dogs. *Nat Genet* 2011;43:72–78.
23 Heuser T, Raytchev M, Krell J, Porter ME, Nicastro D. The dynein regulatory complex is the nexin link and a major regulatory node in cilia and flagella. *J Cell Biol* 2009;187:921–933.
24 Dunican EM, Elicker BM, Henry T, Gierada DS, Schiebler ML, Anderson W, *et al.* Mucus plugs and emphysema in the pathophysiology of airflow obstruction and hypoxemia in smokers. *Am J Respir Crit Care Med* 2021;203:957–968.
25 Mummy DG, Dunican EM, Carey KJ, Evans MD, Elicker BM, Newell JD Jr, *et al.* Mucus plugs in asthma at CT associated with regional ventilation defects at 3He MRI. *Radiology* 2022;303:184–190.
26 Dunican EM, Elicker BM, Gierada DS, Nagle SK, Schiebler ML, Newell JD, *et al.* Mucus plugs in patients with asthma linked to eosinophilia and airflow obstruction. *J Clin Invest* 2018;128: 997–1009.
27 Tang M, Elicker BM, Henry T, Gierada DS, Schiebler ML, Huang BK, *et al.* Mucus plugs persist in asthma, and changes in mucus plugs associate with changes in airflow over time. *Am J Respir Crit Care Med* 2022;205:1036–1045.
28 Lachowicz-Scroggins ME, Yuan S, Kerr SC, Dunican EM, Yu M, Carrington SD, *et al.* Abnormalities in MUC5AC and MUC5B protein in airway mucus in asthma. *Am J Respir Crit Care Med* 2016;194: 1296–1299.
29 Shah A, Shoemark A, MacNeill SJ, Bhaludin B, Rogers A, Bilton D, *et al.* A longitudinal study characterising a large adult primary ciliary dyskinesia population. *Eur Respir J* 2016;48:441–450.
30 Jain K, Padley SP, Goldstraw EJ, Kidd SJ, Hogg C, Biggart E, *et al.* Primary ciliary dyskinesia in the paediatric population: range and severity of radiological findings in a cohort of patients receiving tertiary care. *Clin Radiol* 2007;62:986–993.
31 Hoang-Thi TN, Revel MP, Burgel PR, Bassinet L, Honoré I, Hua-Huy T, *et al.* Automated computed tomographic scoring of lung disease in adults with primary ciliary dyskinesia. *BMC Pulm Med* 2018; 18:194.
32 Cohen-Cymberknoh M, Simanovsky N, Hiller N, Hillel AG, Shoseyov D, Kerem E. Differences in disease expression between primary ciliary dyskinesia and cystic fibrosis with and without pancreatic insufficiency. *Chest* 2014;145:738–744.
33 Rosenow T, Mok LC, Turkovic L, Berry LJ, Sly PD, Ranganathan S, *et al.* The cumulative effect of inflammation and infection on structural lung disease in early cystic fibrosis. *Eur Respir J* 2019;54: 1801771.
34 Tiddens H, Chen Y, Andrinopoulou ER, Davis SD, Rosenfeld M, Ratjen F, *et al.* The effect of inhaled hypertonic saline on lung structure in children aged 3–6 years with cystic fibrosis (SHIP-CT): a multicentre, randomised, double-blind, controlled trial. *Lancet Respir Med* 2022;10: 669–678.